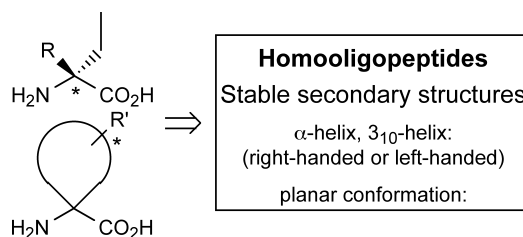


Contents

Review

Design and Synthesis of Chiral α,α -Disubstituted Amino Acids and Conformational Study of Their Oligopeptides

M. Tanaka

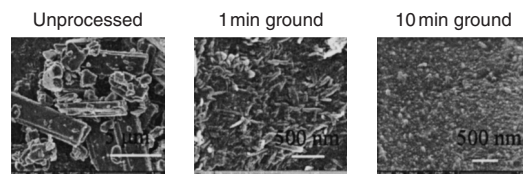


pp. 349–358

Regular Articles

Preparation of Drug Nanoparticles by Co-grinding with Cyclodextrin: Formation Mechanism and Factors Affecting Nanoparticle Formation

A. Wongmekiat, Y. Tozuka, K. Moribe, T. Oguchi, and K. Yamamoto

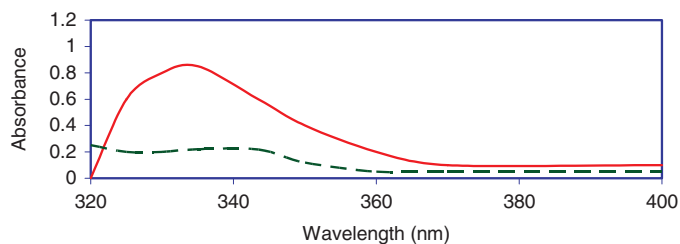


Particle size reduction of pranlukast after grinding with β -Cyclodextrin

pp. 359–363

Spectrophotometric and Spectrofluorimetric Methods for the Determination of Tranexamic Acid in Pharmaceutical Formulation

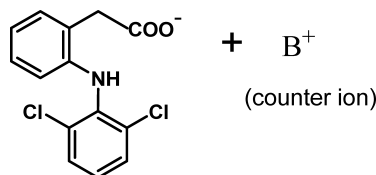
K. A. El-Aroud, A. M. Abushoffa, and H. E. Abdellatef



pp. 364–367

Enhanced Skin Permeation of Diclofenac by Ion-Pair Formation and Further Enhancement by Microemulsion

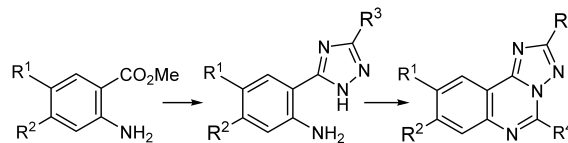
M. A. H. M. Kamal, N. Iimura, T. Nabekura, and S. Kitagawa



pp. 368–371

Synthesis and Evaluation of Adenosine Antagonist Activity of a Series of [1,2,4]Triazolo[1,5-c]quinazolines

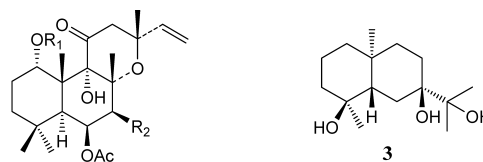
C. Balo, C. López, J. M. Brea, F. Fernández, and O. Caamaño



pp. 372–375

Two Minor Diterpene Glycosides and an Eudesman Sesquiterpene from *Coleus forskohlii*

Y. Shan, X. Wang, X. Zhou, L. Kong, and M. Niwa

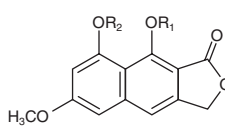


1 R_1 =Glc R_2 =OH
2 R_1 =Glc R_2 =OAc

pp. 376–381

Antioxidative Effects of 6-Methoxysorigenin and Its Derivatives from *Rhamnus nakaharai*

L.-T. Ng, C.-C. Lin, and C.-M. Lu



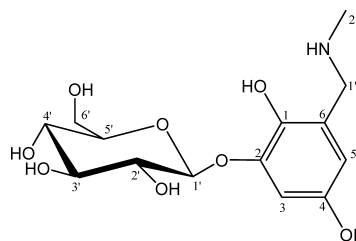
2: $R_1=R_2=H$
2a: $R_1=R_2=COCH_3$
2b: $R_1=R_2=COCH_2CH_3$
3: $R_1=H, R_2=Glc$
4: $R_1=H, R_2=Glc-Xyl$
5: $R_1=H, R_2=Rutinose$

6-Methoxysorigenin (2) exhibits potent antioxidative activities as evaluated by DPPH radical-scavenging, metal chelating, TBARS elimination, and ESR methods.

pp. 382–384

Mutagenic, Antimutagenic and Antioxidant Activities of a New Class of β -Glucoside Hydroxyhydroquinone from *Anagallis monelli* Growing in Tunisia

S. Ammar, M. A. Mahjoub, N. Charfi, I. Skandarani, L. Chekir-Ghedira, and Z. Mighri

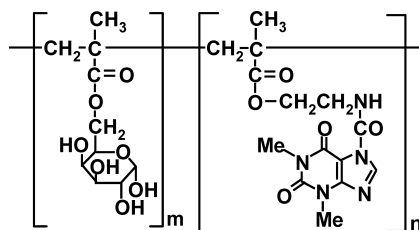


Zinolol

pp. 385–388

Conventional Synthesis of Amphiphilic Block Copolymer Utilized for Polymeric Micelle by Mechanochemical Solid-State Polymerization

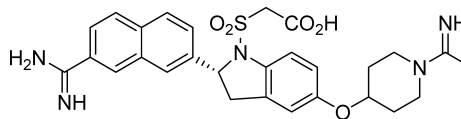
S. Kondo, H. Mori, Y. Sasai, and M. Kuzuya



pp. 389–392

Indoline Derivatives II: Synthesis and Factor Xa (FXa) Inhibitory Activities

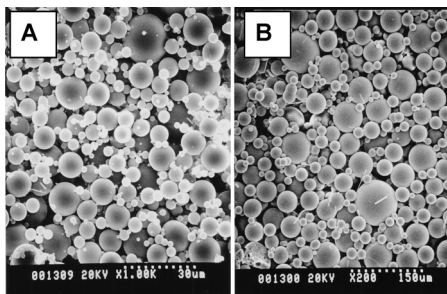
T. Noguchi, N. Tanaka, T. Nishimata, R. Goto, M. Hayakawa, A. Sugidachi, T. Ogawa, F. Asai, T. Ozeki, and K. Fujimoto



pp. 393–402

A Novel Preparation Method for Microspheres of Water Soluble Polymers Using Polypropyleneglycol as the Dispersion Medium

T. Seki, K. Shinohara, N. Kato, M. Uchida, H. Natsume, K. Morimoto, and K. Juni

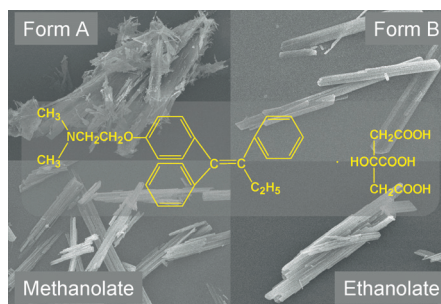


Initial temperature of PPG
A; 20°C
B; 30°C
 (PPG–Aqueous Phase=93.3:6.7)

pp. 403–406

Physicochemical Characterization of Tamoxifen Citrate Pseudopolymorphs, Methanolate and Ethanolate

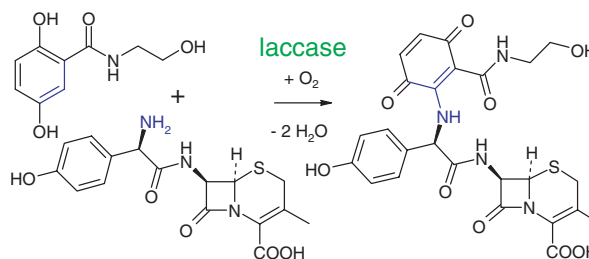
T. Kojima, F. Kato, R. Teraoka, Y. Matsuda, S. Kitagawa, and M. Tshako



pp. 407–411

Novel Cephalosporins Synthesized by Amination of 2,5-Dihydroxybenzoic Acid Derivatives Using Fungal Laccases II

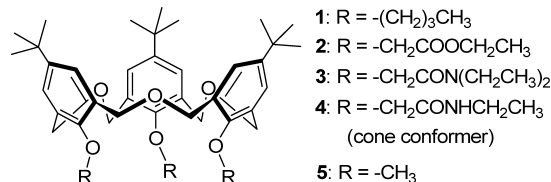
A. Mikolasch, T. H. J. Niedermeyer, M. Lalk, S. Witt, S. Seefeldt, E. Hammer, F. Schauer, M. Gesell Salazar, S. Hessel, W.-D. Jülich, and U. Lindequist



pp. 412–416

The Effects of *O*-Substituents of Hexahomotrioxacalix[3]arene on Potentiometric Discrimination between Dopamine and Biological Organic/Inorganic Cations

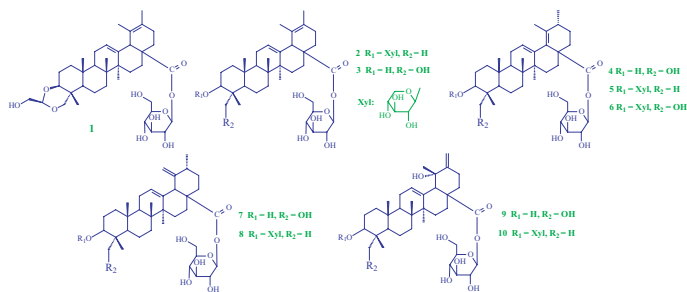
R. Saijo, H. Murakami, S. Tsunekawa, S. Imanishi, N. Shirai, S. Ikeda, and K. Odashima



pp. 417–421

Six New Triterpenoid Saponins from the Leaves of *Ilex oblonga* and Their Inhibitory Activities against TMV Replication

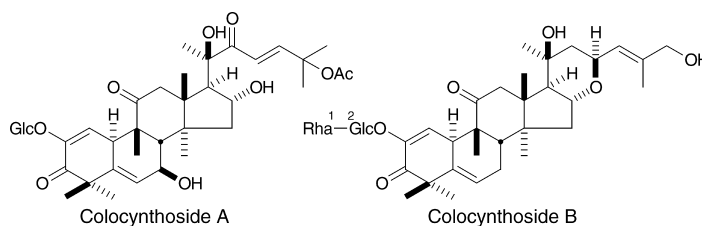
Z.-J. Wu, M.-A. Ouyang, C.-Z. Wang, and Z.-K. Zhang



pp. 422–427

Bioactive Saponins and Glycosides. XXVII. Structures of New Cucurbitane-Type Triterpene Glycosides and Antiallergic Constituents from *Citrullus colocynthis*

M. Yoshikawa, T. Morikawa, H. Kobayashi, A. Nakamura, K. Matsuhira, S. Nakamura, and H. Matsuda

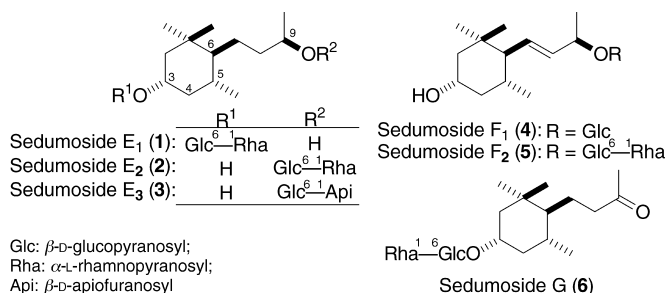


Glc: β -D-glucopyranosyl; Rha: α -L-rhamnopyranosyl

pp. 428–434

Bioactive Constituents from Chinese Natural Medicines. XXII. Absolute Structures of New Megastigmane Glycosides, Sedumosides E₁, E₂, E₃, F₁, F₂, and G, from *Sedum sarmentosum* (Crassulaceae)

T. Morikawa, Y. Zhang, S. Nakamura, H. Matsuda, O. Muraoka, and M. Yoshikawa

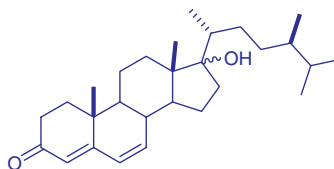


pp. 435–441

Notes

Glutathione *S*-Transferase Inhibiting Chemical Constituents of *Caesalpinia bonduc*

C. C. Udenigwe, A. Ata, and R. Samarasekera

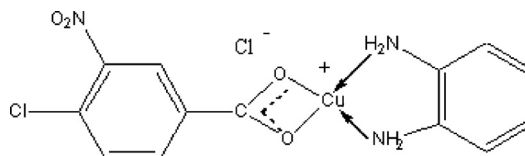


Glutathione *S*-transferase (GST) assay-directed fractionations of the ethanolic extracts of *Caesalpinia bonduc* yielded one new sterol, 17-hydroxycampesta-4,6-dien-3-one (1), two known 13,14-*seco*-sterols, one known cassane furanoditerpene as well as one known aromatic dioxane, as the active compounds. GST inhibitory activity of the isolated compounds was compared with sodium taurocholate, a standard GST inhibitor.

pp. 442–445

Preparation and Antibacterial Activity of Copper and Cobalt Complexes of 4-Chloro-3-nitrobenzoate with a Nitrogen Donor Ligand

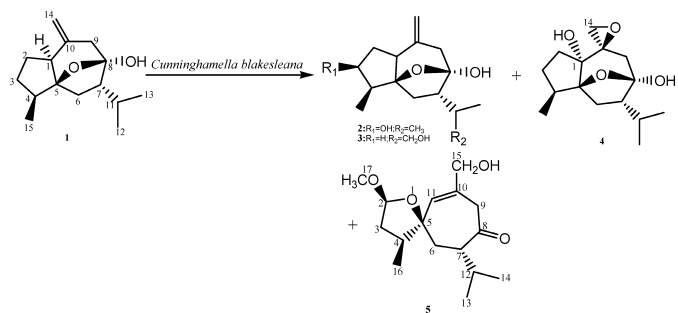
A. T. Kabbani, H. H. Hammud, and A. M. Ghannoum



pp. 446–450

Four Novel Metabolites from Microbial Transformation of Curcumol by *Cunninghamella blakesleana*

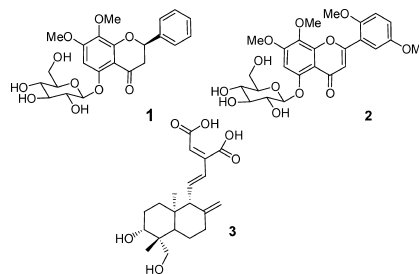
H. Zhang, N. Kang, F. Qiu, G. Qu, and X. Yao



pp. 451–454

Secondary Metabolites from *Andrographis paniculata*

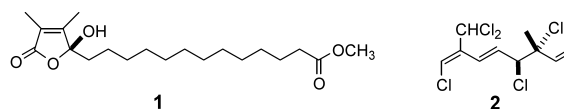
W. Li, X. Xu, H. Zhang, C. Ma, H. Fong, R. van Breemen, and J. Fitzloff



pp. 455–458

A New 2,3-Dimethyl Butenolide from the Brittle Star *Ophiomastix mixta*

J. Lee, W. Wang, J. Hong, C.-O. Lee, S. Shin, K. S. Im, and J. H. Jung

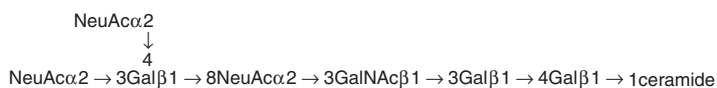


A new butenolide (1) was isolated, along with a known acyclic polyhalogenated monoterpene (2), from the brittle star *Ophiomastix mixta*. The compounds were tested for cytotoxicity against a panel of five human solid tumor cell lines and displayed mild to significant activity.

pp. 459–461

Neuritogenic Activity of Gangliosides from Echinoderms and Their Structure–Activity Relationship

M. Kaneko, K. Yamada, T. Miyamoto, M. Inagaki, and R. Higuchi

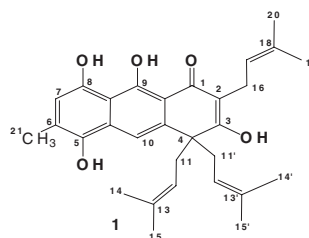


SJG-2, ganglioside from sea cucumber, possessing most potent activity

pp. 462–463

Anti-plasmodial Activity of Some Constituents of the Root Bark of *Harungana madagascariensis* LAM. (Hypericaceae)

B. Ndjakou Lenta, S. Ngouela, F. Fekam Boyom, F. Tantangmo, G. R. Feuya Tchouya, E. Tsamo, J. Gut, P. J. Rosenthal, and J. Donald Connolly

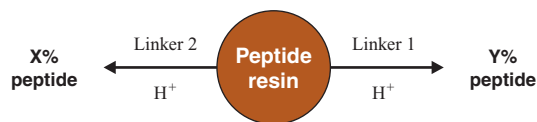


Compound 1 showed a potent antiplasmodial activity (1.80 μM).

pp. 464–467

Comparative Investigation of the Cleavage Step in the Synthesis of Model Peptide Resins: Implications for N^{α} -9-Fluorenylmethyl-oxycarbonyl-Solid Phase Peptide Synthesis

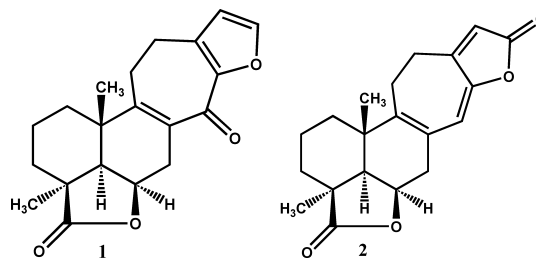
G. N. Jubilut, E. M. Cilli, E. Crusca, Jr., E. H. Silva, Y. Okada, and C. R. Nakaie



pp. 468–470

Two New Rare-Class Tetracyclic Diterpenoids from *Otostegia limbata*

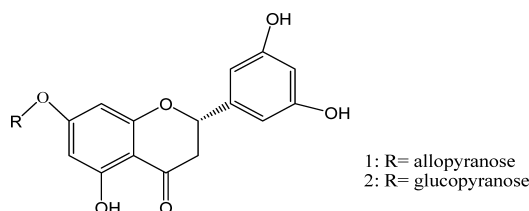
U. Farooq, A. Khan, V. U. Ahmad, S. S. Khan, F. Kousar, and S. Arshad



pp. 471–473

Two New Flavanone Glycosides of *Jasminum lanceolarium* and Their Anti-oxidant Activities

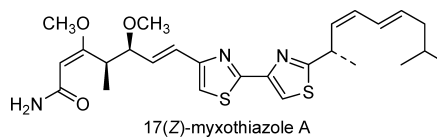
J.-M. Sun, J.-S. Yang, and H. Zhang



pp. 474–476

Bithiazole Metabolites from the *Myxobacterium Myxococcus fulvus*

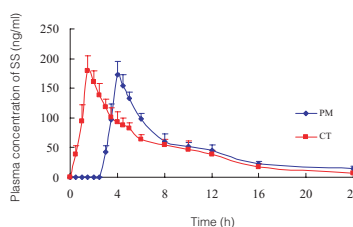
J.-W. Ahn, K. H. Jang, H.-C. Yang, K.-B. Oh, H.-S. Lee, and J. Shin



pp. 477–479

The Investigation of the Pharmacokinetics of Pulsatile-Release Salbutamol Sulfate with pH-Sensitive Ion Exchange Resin as the Carriers in Beagle Dogs

H. Liu, T. Sun, F. Yu, X. Zhao, H. Guo, and W. Pan

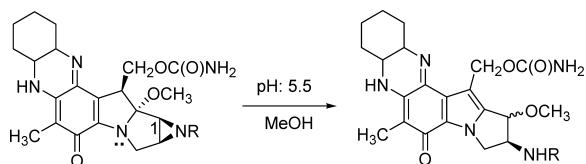


In the present study, we investigated the pharmacokinetics of the salbutamol sulfate pulsatile-release capsules in beagle dogs. The pharmacokinetics parameters of pulsatile-release salbutamol sulfate and reference tablet were AUC_{0-24} (ng·h/ml) 1031.8 ± 123.1 , 1112.6 ± 1182.4 , C_{max} (ng/ml) 172.4 ± 21.4 , 179.3 ± 26.1 , T_{max} (h) 3.8 ± 0.6 , 1.5 ± 0.5 , T_{lag} (h) 2.7 ± 0.5 , 0.3 ± 0.2 . The results showed that the test dosage forms was bio-equivalent with reference dosage form, and had an obviously pulsatile-release effect.

pp. 480–481

Solvolytic Study of Cycliciminomitomycins

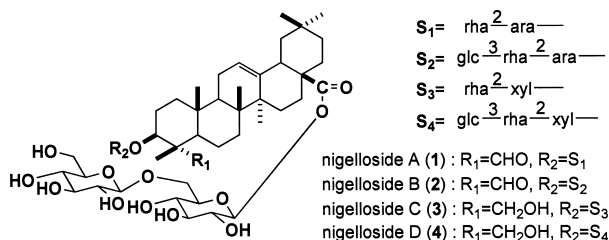
Y. Na



pp. 482–487

Four New Triterpene Glycosides from *Nigella damascena*

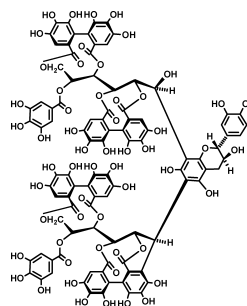
H. Yoshimitsu, M. Nishida, M. Okawa, and T. Nohara



pp. 488–491

Cowaniin, a C-Glucosidic Ellagitannin Dimer Linked through Catechin from *Cowania mexicana*

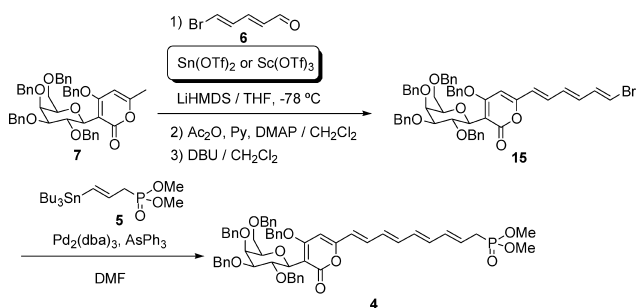
H. Ito, M. Miyake, E. Nishitani, K. Miyashita, M. Yoshimura, T. Yoshida, M. Takasaki, T. Konoshima, M. Kozuka, and T. Hatano



pp. 492–494

Synthetic Study on Telomerase Inhibitor, D8646-2-6: Synthesis of the Key Intermediate Using $\text{Sn}(\text{OTf})_2$ or $\text{Sc}(\text{OTf})_3$ Mediated Aldol-Type Reaction and Stille Coupling

A. Kanai, Y. Takeda, K. Kuramochi, A. Nakazaki, and S. Kobayashi

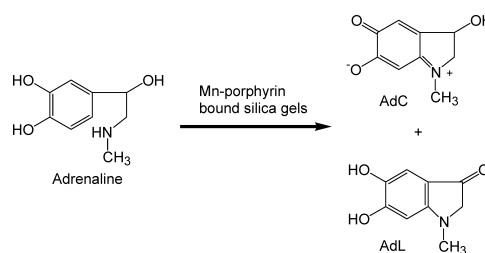


pp. 495–499

Communications to the Editor

Catalytic Activity of Silica Gels Bound Manganese(III)–Porphyrin on Oxidative Reaction of Adrenaline

Y. Kitamura, T. Takatsuki, M. Kawamoto, M. Saito, A. Iwado, I. Tsukamoto, M. Mifune, and Y. Saito



pp. 500–502

About the cover: ORIGAMI, the Japanese art of paper folding, is one traditional pastime in Japanese culture, and it is also well-known as one aspect of Japanese beauty throughout the world. Colorful flat square pieces of paper are folded eloquently into ORIGAMIs such as a TSURU (crane), YAKKOSAN (person), KABUTO (traditional warriors helmet), NINJA fighting star, FUSEN (balloon), and SARA (dish) as shown in the cover picture (clockwise from crane). Also, oligopeptides composed of chiral α,α -disubstituted amino acids have a strong tendency to adopt specific compact conformations (planer, 3_{10} -helix, and α -helix), though they are inferior to the ORIGAMI. The cover picture shows a regularly folded left-handed 3_{10} -helix (left side) and a left-handed α -helix (right side) of oligomers that consist of chiral cyclic α,α -disubstituted amino acids having side-chain chiral centers. See the review by Tanaka on page 349 of this issue.